



A highly accurate wavelet approach for multi-term variable-order fractional multi-dimensional differential equations

Haniye Dehestani and Yadollah Ordokhani*

Department of Mathematics, Faculty of Mathematical Sciences, Alzahra University, Tehran, Iran.

Abstract

In this work, the multi-term variable-order fractional multi-dimensional differential equations are studied based on Gegenbauer wavelet functions. The main aim of this paper is to develop the spectral method with the help of modified operational matrices, which are directly effective in the numerical process. Therefore, we discuss the novel method of obtaining the modified operational matrices (MOMs) of integration and variable-order (VO) fractional derivative. Then, the overall algorithm for solving multi-term VO-fractional differential equations and partial differential equations is introduced. We also discuss error analysis in detail. At last, we implement the numerical scheme in several examples that involve the damped mechanical oscillator equation, the VO-fractional mobile-immobile advection-dispersion equation, and the VO-fractional nonlinear Galilei invariant advection-diffusion equation. Also, to confirm the theoretical results and demonstrate the accuracy and efficiency of the method, we compare our numerical results with analytical solutions and other existing methods.

Keywords. Gegenbauer wavelet functions, Modified operational matrix, Transformation matrix, Variable-order fractional derivative, Partial differential equations.

2010 Mathematics Subject Classification. 34A08, 65T60.

1. INTRODUCTION

In recent years, fractional derivative and integral operators have attracted considerable attention from researchers in many fields of science and engineering (see [7–9, 22, 30, 33] and references therein).

For the first time, Samko and Ross [34] suggested the concepts of variable-order fractional differentiation and integration by extending the use and the notion of the constant-order fractional derivative. Many researchers have studied the application of fractional derivatives in various sciences. Here, we mention some of them: modeling linear and nonlinear oscillators with viscoelastic damping [15], modeling of diffusive–convective effects on the oscillatory flows [31], processing of geographical data [16], and many others, which can be observed in [11, 32, 35, 37, 42].

Recently, numerous researchers have been working diligently to design and analyze numerical solutions for variable-order constant-order fractional problems. For instance, Li and Wu [29] introduced a new reproducing kernel method for variable-order fractional boundary value problems. Yaghoobi et al. [41] employed cubic spline approximation for variable-order fractional differential equations with time delay. Jia et al. [28] developed a fast divided-and-conquer indirect collocation method for variable-order space-fractional diffusion equations. Dehestani et al. [18] applied fractional-order Bessel wavelet functions for solving variable-order fractional optimal control problems. Heydari et al. [26] constructed an operational matrix method for the nonlinear variable-order time fractional reaction-diffusion equation involving the Mittag-Leffler kernel. Authors in [19] utilized the Mott-fractional Mott functions for finding the solution of fractional partial integro-differential viscoelastic equations with weakly singular kernel. Arqub and Maayah [3] employed a reproducing kernel computational approach for time-fractional mobile-immobile advection-dispersion equations. For more information, see [4, 5].

Received: 12 August 2024 ; Accepted: 08 October 2024.

* Corresponding author. Email: ordokhani@alzahra.ac.ir.

In recent years, numerical studies of multi-term variable-order (MT-VO) fractional partial differential equations have appeared in the literature, such as discrete scheme based on Genocchi polynomials and fractional Laguerre functions [20], an optimization wavelet method [27], the Legendre wavelets method [12], a collocation method based on shifted Legendre polynomials [23], and so on.

This paper focuses on the numerical solution of multi-term variable-order fractional partial differential equations. Also, to demonstrate the applicability of the proposed method in real-life problems, we solve the damped mechanical oscillator equation, mobile-immobile advection-dispersion equation, and nonlinear Galilei invariant advection-diffusion equation [1, 2, 40, 43].

Orthogonal functions have attracted the consideration of many mathematicians for approximating the solution of the problems arising from science and engineering. The main reason for using these functions in solving the problems is that these functions easily transfer the problem under study to a system of linear or nonlinear algebraic equations. The reason given became a motivating factor to use Gegenbauer wavelet functions [38] for solving multi-term variable-order fractional partial differential equations.

1.1. A concise literature review for the wavelet method. The theory of wavelets has attracted the attention of many investigators in recent years. Wavelets are a really powerful tool for solving a wide range of problems in physics and engineering disciplines, such as signal analysis and image processing [17].

The wavelet basis functions have many advantages over other basis functions, and they can be implemented in many problems that can not be solved by analytical methods. It is worth mentioning here that these functions have many significant advantages: orthogonality, arbitrary regularity, and good localization [13].

Due to the theory of wavelet functions, many wavelet functions have been introduced to approximate the solution of problems. For example, Chebyshev wavelet functions [27], sine-cosine wavelet functions [36], Haar wavelet functions [6, 25], fractional-order Alpert multiwavelet functions [24], Legendre wavelet functions [12], and fractional-order Bessel wavelet functions [18].

In this paper, we concentrate on describing the discretization methods based on Gegenbauer wavelet functions (GWFs). These functions have been constructed by shifted Gegenbauer polynomials (SGPs) [21, 39], which inherit some of the features of these polynomials. Also, we introduce the method to calculate the components of modified operational matrices of integration and VO-fractional derivative, which play a significant role in numerical algorithms. The advantages of the current approach are listed as follows:

- The accurate integral operational matrix of GWFs is computed.
- Achieving a highly accurate approximate solution and satisfactory results requires leveraging the low values of the Gegenbauer wavelet functions.
- The operational matrices are more accurate in comparison to the operational matrix obtained by the usual methods, and this feature causes us to get the approximate solution with high precision.

The layout of the paper is as follows: The Gegenbauer wavelet functions and some properties of them are introduced in section 2. In section 3 a novel method to describe the elements of the modified operational matrix of integration is proposed. Section 4 is devoted to computing the modified operational matrix of the fractional derivative. The numerical scheme for solving MT-VO-fractional differential equations and MT-VO-fractional partial differential equations is described in detail in section 5. Section 6 investigates the error estimation of the method in Sobolev space. In section 7, we implement the numerical algorithms for several test problems. Section 8 gives a brief conclusion.

1.2. General form of problem statement. In this paper, we focus on the new numerical technique to obtain the approximate solution of the following equations:

Problem 1: Multi-term variable-order fractional differential equations

$$\mathcal{F} \left(t, u(t), u'(t), D^{\nu(t)} u(t), D^{\gamma(t)} u(t) \right) = f(t), \quad 1 < \nu(t) \leq 2, \quad 0 < \gamma(t) \leq 1, \quad (1.1)$$

with the initial conditions

$$u(0) = a_0, \quad u'(0) = a_1,$$

where $D^{\nu(t)}$ and $D^{\gamma(t)}$ denote the Caputo fractional derivatives of the variable-order [20].



Problem 2: Multi-term variable-order fractional partial differential equations

$$\mathcal{H} \left(x, t, u(x, t), \frac{\partial u(x, t)}{\partial x}, \frac{\partial^2 u(x, t)}{\partial x^2}, D_t^{\nu(x,t)} u(x, t), D_t^{\gamma(x,t)} u(x, t), D_t^{\vartheta(x,t)} \left(\frac{\partial^2 u(x, t)}{\partial x^2} \right) \right) = h(x, t), \tag{1.2}$$

$$0 < \nu(x, t), \gamma(x, t), \vartheta(x, t) \leq 1,$$

subject to the initial and boundary conditions

$$u(x, 0) = \varphi(x), \quad u(0, t) = \rho_0(t), \quad u(1, t) = \rho_1(t), \quad x \in [0, 1], \quad t \in [0, 1].$$

Here, $D_t^{\nu(x,t)}$, $D_t^{\gamma(x,t)}$, and $D_t^{\vartheta(x,t)}$ denote the Caputo fractional derivatives of the variable-order [20]. The general form of the proposed derivative of order $q - 1 < \mu(x, t) \leq q$ with respect to variable t is defined as follows [20]:

$$D_t^{\mu(x,t)} u(x, t) = \begin{cases} \frac{1}{(q-\mu(x,t))} \int_0^t (t-s)^{q-\mu(x,t)-1} \frac{\partial^q u(x,s)}{\partial s^q} ds, & q-1 < \mu(x,t) < q, \\ \frac{\partial^q u(x,t)}{\partial t^q}, & \mu(x,t) = q \in \mathbb{N}. \end{cases}$$

2. GEGENBAUER WAVELET FUNCTIONS

The Gegenbauer wavelet functions over the interval $[0, 1)$ are defined by the following formula [38]:

$$\Psi_{nm}(x) = \begin{cases} 2^{\frac{\mathcal{K}-1}{2}} \tilde{G}_m^\lambda (2^{\mathcal{K}-1}x - n + 1), & \frac{n-1}{2^{\mathcal{K}-1}} \leq x < \frac{n}{2^{\mathcal{K}-1}}, \\ 0, & \text{otherwise,} \end{cases} \quad m = 0, 1, \dots, \mathcal{M}, \quad n = 1, 2, \dots, 2^{\mathcal{K}-1}, \tag{2.1}$$

where \mathcal{K} is any positive integer. Furthermore

$$\tilde{G}_m^\lambda (2^{\mathcal{K}-1}x - n + 1) = \frac{1}{\sqrt{\frac{(\Gamma(\lambda+\frac{1}{2}))^2 \Gamma(m+2\lambda)}{(\Gamma(2\lambda))^2 (2m+2\lambda)m!}}} G_m^\lambda (2^{\mathcal{K}-1}x - n + 1). \tag{2.2}$$

In the above formula, $G_m^\lambda(x)$ denotes the Gegenbauer polynomials of order m , which are defined as follows [38]:

$$G_m^\lambda(x) = \frac{\Gamma(\lambda + \frac{1}{2})}{\Gamma(2\lambda)} \sum_{k=0}^m \frac{(-1)^{m-k} \Gamma(m+k+2\lambda)}{\Gamma(k+\lambda+\frac{1}{2})(m-k)!k!} x^k, \quad m = 0, 1, \dots, \mathcal{M}. \tag{2.3}$$

In addition, the Gegenbauer polynomials are orthogonal with respect to the weight function $\omega^\lambda(x) = (x - x^2)^{\lambda-\frac{1}{2}}$ on the interval $[0, 1)$. So that

$$\int_0^1 \omega^\lambda(x) G_m^\lambda(x) G_n^\lambda(x) dx = \begin{cases} 0, & m \neq n, \\ h_m^\lambda, & m = n, \end{cases} \quad m, n = 0, 1, \dots, \mathcal{M},$$

where

$$h_m^\lambda = \frac{(\Gamma(\lambda + \frac{1}{2}))^2 \Gamma(m + 2\lambda)}{(\Gamma(2\lambda))^2 (2m + 2\lambda)m!}.$$

We also demonstrate the curve of GWFs with $\mathcal{M} = \mathcal{K} = 2$ in Figure 1.

2.1. Function approximation. Any square integrable function $f(x)$ can be expanded by Gegenbauer wavelet functions over the interval $[0, 1)$ as follows:

$$f(x) \simeq \sum_{n=1}^{2^{\mathcal{K}-1}} \sum_{m=0}^{\mathcal{M}} f_{nm} \Psi_{nm}(x) = F^T \Psi(x), \tag{2.4}$$

where

$$F = [f_{10}, f_{11}, \dots, f_{1\mathcal{M}} | f_{20}, f_{21}, \dots, f_{2\mathcal{M}} | \dots | f_{2^{\mathcal{K}-1}0}, f_{2^{\mathcal{K}-1}1}, \dots, f_{2^{\mathcal{K}-1}\mathcal{M}}]^T,$$

and

$$\Psi(x) = [\Psi_{10}(x), \Psi_{11}(x), \dots, \Psi_{1\mathcal{M}}(x) | \dots | \Psi_{2^{\mathcal{K}-1}0}(x), \Psi_{2^{\mathcal{K}-1}1}(x), \dots, \Psi_{2^{\mathcal{K}-1}\mathcal{M}}(x)]^T.$$



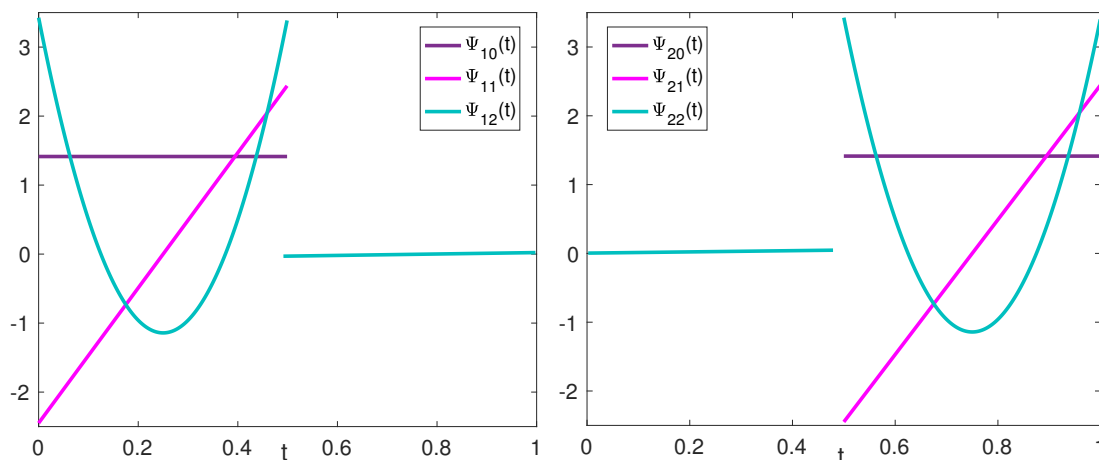


FIGURE 1. The curve of the GWFs with $\mathcal{M} = \mathcal{K} = 2$.

Each component of the vector F can be calculated according to the following relation:

$$f_{nm} = \int_0^1 \omega^\lambda (2^{\mathcal{K}-1}x - n + 1) f(x) \Psi_{nm}(x) dx, \quad m = 0, 1, \dots, \mathcal{M}, \quad n = 1, 2, \dots, 2^{\mathcal{K}-1}.$$

2.2. Transformation matrix from GWFs to SGPs. The current part provides the transformation matrix from GWFs to SGPs:

$$\Psi_{2^{\mathcal{K}-1}(\mathcal{M}+1) \times 1}(x) = \Theta_{2^{\mathcal{K}-1}(\mathcal{M}+1) \times (\mathcal{M}+1)} G_{(\mathcal{M}+1) \times 1}^\lambda(x), \tag{2.5}$$

where

$$\Theta = \begin{cases} \Theta_1, & 0 \leq x < \frac{1}{2^{\mathcal{K}-1}}, \\ \Theta_2, & \frac{1}{2^{\mathcal{K}-1}} \leq x < \frac{2}{2^{\mathcal{K}-1}}, \\ \vdots \\ \Theta_{2^{\mathcal{K}-1}}, & \frac{2^{\mathcal{K}-1}-1}{2^{\mathcal{K}-1}} \leq x < 1, \end{cases}$$

is called the transformation matrix. So that, the components of the proposed matrix is design as follows:

$$\Theta_n = \begin{bmatrix} O & O & \dots & \underbrace{\tilde{\Theta}_n}_{\text{defined on } [\frac{n-1}{2^{\mathcal{K}-1}}, \frac{n}{2^{\mathcal{K}-1}}]} & \dots & O & O \end{bmatrix}^T, \quad n = 1, 2, \dots, 2^{\mathcal{K}-1},$$

where O denotes the zero matrix with $(\mathcal{M} + 1) \times (\mathcal{M} + 1)$ dimension. In a particular case, for $\mathcal{M} = 2, \mathcal{K} = 2$ and $\lambda = 1$, we have

$$\left. \begin{aligned} \Psi_{10}(x) &= \sqrt{2} = \sqrt{2}G_0^1(x), \\ \Psi_{11}(x) &= 4\sqrt{6}x - \sqrt{6} = \sqrt{6}G_0^1(x) + \sqrt{6}G_1^1(x), \\ \Psi_{12}(x) &= 64\sqrt{\frac{30}{23}}x^2 - 32\sqrt{\frac{30}{23}}x + 3\sqrt{\frac{30}{23}} = 63\sqrt{\frac{30}{23}}G_0^1(x) - 24\sqrt{\frac{30}{23}}G_1^1(x) + 4\sqrt{\frac{30}{23}}G_2^1(x), \end{aligned} \right\} 0 \leq x < \frac{1}{2},$$

and

$$\left. \begin{aligned} \Psi_{20}(x) &= \sqrt{2} = \sqrt{2}G_0^1(x), \\ \Psi_{21}(x) &= 4\sqrt{6}x - 3\sqrt{6} = -\sqrt{6}G_0^1(x) + \sqrt{6}G_1^1(x), \\ \Psi_{22}(x) &= 64\sqrt{\frac{30}{23}}x^2 - 96\sqrt{\frac{30}{23}}x + 35\sqrt{\frac{30}{23}} = 127\sqrt{\frac{30}{23}}G_0^1(x) - 40\sqrt{\frac{30}{23}}G_1^1(x) + 4\sqrt{\frac{30}{23}}G_2^1(x), \end{aligned} \right\} \frac{1}{2} \leq x < 1.$$



Then, the transformation matrix is calculated as follows:

$$\Theta = \begin{cases} \Theta_1, & 0 \leq x < \frac{1}{2}, \\ \Theta_2, & \frac{1}{2} \leq x < 1, \end{cases}$$

where

$$\Theta_1 = \begin{bmatrix} \sqrt{2} & 0 & 0 \\ \sqrt{6} & \sqrt{6} & 0 \\ 63\sqrt{\frac{30}{23}} & -24\sqrt{\frac{30}{23}} & 4\sqrt{\frac{30}{23}} \\ 0 & 0 & 0 \\ 0 & 0 & 0 \\ 0 & 0 & 0 \end{bmatrix}, \quad \Theta_2 = \begin{bmatrix} 0 & 0 & 0 \\ 0 & 0 & 0 \\ 0 & 0 & 0 \\ \sqrt{2} & 0 & 0 \\ -\sqrt{6} & \sqrt{6} & 0 \\ 127\sqrt{\frac{30}{23}} & -40\sqrt{\frac{30}{23}} & 4\sqrt{\frac{30}{23}} \end{bmatrix}.$$

3. THE MODIFIED OPERATIONAL MATRIX OF INTEGRATION

In this section, we improve the technique of calculating the operational matrix of integration. First, we obtain the modified operational matrix of integration for SGPs. Then, according to the transformation matrix, we introduce a modified operational matrix of integration for GWFs. To achieve the desired purpose, we consider

$$\int_0^x G^\lambda(\xi)d\xi = \Upsilon G^\lambda(x) + \Delta(x). \tag{3.1}$$

Here, Υ is called a modified operational matrix, and $\Delta(x)$ is the complement vector. In order to obtain the elements of the modified operational matrix and the complement vector, we use the analytical form of SGPs as follows:

$$\int_0^x G_m^\lambda(\xi)d\xi = \int_0^x \frac{\Gamma(\lambda + \frac{1}{2})}{\Gamma(2\lambda)} \sum_{k=0}^m \frac{(-1)^{m-k}\Gamma(m+k+2\lambda)}{\Gamma(k+\lambda+\frac{1}{2})(m-k)!k!} \xi^k d\xi = \sum_{k=0}^m \delta_{m,k}^\lambda x^{k+1}, \tag{3.2}$$

where

$$\delta_{m,k}^\lambda = \frac{\Gamma(\lambda + \frac{1}{2})}{\Gamma(2\lambda)} \frac{(-1)^{m-k}\Gamma(m+k+2\lambda)}{\Gamma(k+\lambda+\frac{1}{2})(m-k)!(k+1)!}.$$

To go on with the process of the method, we need to expand x^{k+1} by SGPs. Hence, we have

$$x^{k+1} = \sum_{i=0}^{\mathcal{M}} a_i G_i^\lambda(x).$$

On the other hand, using the above relation and to prevent the increase of error, we consider

$$\int_0^x G_m^\lambda(\xi)d\xi = \begin{cases} \sum_{i=0}^{\mathcal{M}} \left(\sum_{k=0}^m \eta_{m,k,i}^\lambda \right) G_i^\lambda(x), & m = 0, 1, \dots, \mathcal{M} - 1, \\ \sum_{i=0}^{\mathcal{M}} \left(\sum_{k=0}^{m-1} \eta_{m,k,i}^\lambda \right) G_i^\lambda(x) + \delta_{\mathcal{M},k}^\lambda x^{\mathcal{M}+1}, & m = \mathcal{M}, \end{cases} \tag{3.3}$$

where $\eta_{m,k,i}^\lambda = \delta_{m,k}^\lambda a_i$. Therefore, the general form of the modified operational matrix and the complement vector are gained as follows:

$$\Upsilon = \begin{bmatrix} \eta_{0,0,0}^\lambda & \eta_{0,0,1}^\lambda & \dots & \eta_{0,0,\mathcal{M}}^\lambda \\ \sum_{k=0}^1 \eta_{1,k,0}^\lambda & \sum_{k=0}^1 \eta_{1,k,1}^\lambda & \dots & \sum_{k=0}^1 \eta_{1,k,\mathcal{M}}^\lambda \\ \vdots & \vdots & \ddots & \vdots \\ \sum_{k=0}^{\mathcal{M}-1} \eta_{\mathcal{M}-1,k,0}^\lambda & \sum_{k=0}^{\mathcal{M}-1} \eta_{\mathcal{M}-1,k,1}^\lambda & \dots & \sum_{k=0}^{\mathcal{M}-1} \eta_{\mathcal{M}-1,k,\mathcal{M}}^\lambda \\ \sum_{k=0}^{\mathcal{M}-1} \eta_{\mathcal{M},k,0}^\lambda & \sum_{k=0}^{\mathcal{M}-1} \eta_{\mathcal{M},k,1}^\lambda & \dots & \sum_{k=0}^{\mathcal{M}-1} \eta_{\mathcal{M},k,\mathcal{M}}^\lambda \end{bmatrix}_{(\mathcal{M}+1) \times (\mathcal{M}+1)},$$

and

$$\Delta(x) = [\Delta_m(x)]_{(\mathcal{M}+1) \times 1}, \quad \Delta_m(x) = \begin{cases} 0, & m = 0, 1, \dots, \mathcal{M} - 1, \\ \delta_{\mathcal{M},k}^\lambda x^{\mathcal{M}+1}, & m = \mathcal{M}. \end{cases}$$



For example, for $\mathcal{M} = 2$ and $\lambda = 1$, we get

$$\Upsilon = \begin{bmatrix} 0.5 & 0.25 & 0 \\ -0.375 & 0 & 0.125 \\ -1 & -1.25 & -0.5 \end{bmatrix}, \quad \Delta(x) = \begin{bmatrix} 0 \\ 0 \\ \frac{16}{3}x^3 \end{bmatrix}.$$

Now, with the help of the mentioned process and transformation matrix, we get

$$\begin{aligned} \int_0^x \Psi(\xi)d\xi &= \int_0^x \Theta G^\lambda(\xi)d\xi = \Theta \int_0^x G^\lambda(\xi)d\xi = \Theta (\Upsilon G^\lambda(x) + \Delta(x)) \\ &= \Theta \Upsilon \Theta^{-1} \Psi(x) + \Theta \Delta(x) = \mathbf{Q} \Psi(x) + \Theta \Delta(x), \quad \mathbf{Q} = \Theta \Upsilon \Theta^{-1}. \end{aligned} \tag{3.4}$$

It should be mentioned that to calculate matrix Θ^{-1} , it is sufficient to compute $\tilde{\Theta}^{-1}$. Thus, we have

$$\Theta^{-1} = \begin{cases} \Theta_1^{-1}, & 0 \leq x < \frac{1}{2^{\kappa-1}}, \\ \Theta_2^{-1}, & \frac{1}{2^{\kappa-1}} \leq x < \frac{2}{2^{\kappa-1}}, \\ \vdots \\ \Theta_{2^{\kappa-1}}^{-1}, & \frac{2^{\kappa-1}-1}{2^{\kappa-1}} \leq x < 1, \end{cases}$$

where

$$\Theta_n^{-1} = \begin{bmatrix} O & O & \dots & \underbrace{\tilde{\Theta}_n^{-1}}_{\text{defined on } [\frac{n-1}{2^{\kappa-1}}, \frac{n}{2^{\kappa-1}})} & \dots & O & O \end{bmatrix}^T, \quad n = 1, 2, \dots, 2^{\kappa-1}.$$

According to the above results, we also have the following relation for variable t :

$$\int_0^t \Psi(\eta)d\eta = \bar{\mathbf{Q}} \Psi(t) + \Theta \bar{\Delta}(t). \tag{3.5}$$

4. THE MODIFIED OPERATIONAL MATRIX OF THE VO-FRACTIONAL DERIVATIVE

In this section, the purpose is to compute the modified operational matrix of the fractional derivative of GWFs. First, we obtain the modified operational matrix of the VO-fractional derivative for SGP. Let

$$D_t^{\mu(x,t)} G^\lambda(t) \simeq \frac{\Gamma(\lambda + \frac{1}{2})}{\Gamma(2\lambda)} t^{q-\mu(x,t)} \mathbf{R} G^\lambda(t), \quad q - 1 < \mu(x,t) \leq q. \tag{4.1}$$

Hence, to gain each component of the proposed matrix, we apply the transformation matrix and Eq. (2.3) as follows:

$$\begin{aligned} D_t^{\mu(x,t)} G_m^\lambda(t) &= \frac{\Gamma(\lambda + \frac{1}{2})}{\Gamma(2\lambda)} \sum_{k=0}^m \frac{(-1)^{m-k} \Gamma(m+k+2\lambda)}{\Gamma(k+\lambda+\frac{1}{2})(m-k)!k!} D_t^{\mu(x,t)} (t^k) \\ &= \frac{\Gamma(\lambda + \frac{1}{2})}{\Gamma(2\lambda)} \sum_{k=0}^m \mu_{m,k}^\lambda D_t^{\mu(x,t)} (t^k). \end{aligned} \tag{4.2}$$

In view of the properties of the Caputo variable-order derivative, we have

$$D_t^{\mu(x,t)} t^k = \begin{cases} \frac{\Gamma(k+1)}{\Gamma(k-\mu(x,t)+1)} t^{k-\mu(x,t)}, & k = q, q+1, \dots, \mathcal{M}, \\ 0, & \text{otherwise.} \end{cases}$$

Therefore, it can be deduced that

$$D_t^{\mu(x,t)} G_m^\lambda(t) = \frac{\Gamma(\lambda + \frac{1}{2})}{\Gamma(2\lambda)} \sum_{k=0}^m \beta_{m,k}^\lambda t^{k-\mu(x,t)} = \frac{\Gamma(\lambda + \frac{1}{2})}{\Gamma(2\lambda)} t^{q-\mu(x,t)} \sum_{k=0}^m \beta_{m,k}^\lambda t^{k-q}, \tag{4.3}$$

where

$$\beta_{m,k}^\lambda = \begin{cases} \frac{\Gamma(k+1)}{\Gamma(k-\mu(x,t)+1)} \mu_{m,k}^\lambda, & k = q, q+1, \dots, \mathcal{M}, \\ 0, & \text{otherwise.} \end{cases}$$



Now, by expanding t^{k-q} with respect to SGPs, we conclude

$$t^{k-q} \simeq \sum_{j=0}^{\mathcal{M}} a_j G_j^\lambda(t).$$

By substituting the aforementioned relation in Eq. (4.3), we obtain

$$\begin{aligned} D_t^{\mu(x,t)} G_m^\lambda(t) &= \frac{\Gamma(\lambda + \frac{1}{2})}{\Gamma(2\lambda)} t^{q-\mu(x,t)} \sum_{k=0}^m \beta_{m,k}^\lambda \left(\sum_{j=0}^{\mathcal{M}} a_j G_j^\lambda(t) \right) \\ &= \frac{\Gamma(\lambda + \frac{1}{2})}{\Gamma(2\lambda)} t^{q-\mu(x,t)} \sum_{j=0}^{\mathcal{M}} \left(\sum_{k=0}^m r_{m,k,j}^\lambda \right) G_j^\lambda(t), \end{aligned} \tag{4.4}$$

where $r_{m,k,j}^\lambda = \beta_{m,k}^\lambda a_j$. As a result, from Eq. (4.4), the following relation is obtained:

$$D_t^{\mu(x,t)} G_m^\lambda(t) \simeq \frac{\Gamma(\lambda + \frac{1}{2})}{\Gamma(2\lambda)} t^{q-\mu(x,t)} \left[\sum_{k=0}^m r_{m,k,0}^\lambda \quad \sum_{k=0}^m r_{m,k,1}^\lambda \quad \cdots \quad \sum_{k=0}^m r_{m,k,\mathcal{M}}^\lambda \right] G^\lambda(t).$$

Thus, we have

$$\mathbf{R} = \begin{bmatrix} r_{0,k,0}^\lambda & r_{0,k,1}^\lambda & \cdots & r_{0,k,\mathcal{M}}^\lambda \\ \sum_{k=0}^1 r_{1,k,0}^\lambda & \sum_{k=0}^1 r_{1,k,1}^\lambda & \cdots & \sum_{k=0}^1 r_{1,k,\mathcal{M}}^\lambda \\ \vdots & \vdots & \ddots & \vdots \\ \sum_{k=0}^{\mathcal{M}} r_{\mathcal{M},k,0}^\lambda & \sum_{k=0}^{\mathcal{M}} r_{\mathcal{M},k,1}^\lambda & \cdots & \sum_{k=0}^{\mathcal{M}} r_{\mathcal{M},k,\mathcal{M}}^\lambda \end{bmatrix}.$$

Next, one can derive the modified operational matrix of the fractional derivative of GWFs by using the transformation matrix. Thus, we deduce

$$\begin{aligned} D_t^{\mu(x,t)} \Psi(t) &= \Theta D_t^{\mu(x,t)} (G^\lambda(t)) \simeq \frac{\Gamma(\lambda + \frac{1}{2})}{\Gamma(2\lambda)} t^{q-\mu(x,t)} \Theta \mathbf{R} G^\lambda(t) \\ &= \frac{\Gamma(\lambda + \frac{1}{2})}{\Gamma(2\lambda)} t^{q-\mu(x,t)} \Theta \mathbf{R} \Theta^{-1} \Psi(t) = \frac{\Gamma(\lambda + \frac{1}{2})}{\Gamma(2\lambda)} t^{q-\mu(x,t)} \mathbf{D} \Psi(t), \quad \mathbf{D} = \Theta \mathbf{R} \Theta^{-1}. \end{aligned} \tag{4.5}$$

5. IMPLEMENTATION OF THE NUMERICAL SCHEME

In this section, we discuss the idea of solving the equations mentioned in problems 1 and 2.

5.1. MT-VO-fractional differential equations. This section considers the computational approach for solving MT-VO-fractional differential equations. First, we approximate the second derivative $u''(t)$ by GWFs

$$u''(t) \simeq A^T \Psi(t). \tag{5.1}$$

Now, by integrating Eq. (5.1), we determine the approximation of other functions in Problem 1 as follows:

$$u'(t) \simeq A^T (\bar{\mathbf{Q}} \Psi(t) + \Theta \bar{\mathbf{A}}(t)) + a_1, \tag{5.2}$$

and

$$u(t) \simeq A^T (\bar{\mathbf{Q}}^2 \Psi(t) + \bar{\mathbf{Q}} \Theta \bar{\mathbf{A}}(t) + \Theta W(t)) + a_1 t + a_0, \tag{5.3}$$

where the function $W(t)$ is defined as follows:

$$W(t) = \int_0^t \bar{\mathbf{A}}(\eta) d\eta, \quad W(t) = [W_m(t)], \quad W_m(t) = \begin{cases} 0, & m = 0, 1, \dots, \mathcal{M} - 1, \\ \frac{\delta_{\mathcal{M},k}^\lambda}{\mathcal{M}+2} t^{\mathcal{M}+2}, & m = \mathcal{M}. \end{cases}$$

With the help of the properties of the Caputo VO-fractional derivative and Eq. (5.3), we have

$$D^{\nu(t)} u(t) \simeq A^T \left(\frac{\Gamma(\lambda + \frac{1}{2})}{\Gamma(2\lambda)} t^{2-\nu(t)} \bar{\mathbf{Q}}^2 \mathbf{D} \Psi(t) + \bar{\mathbf{Q}} \Theta Z(t) + \Theta Y(t) \right), \tag{5.4}$$



where

$$Z(t) = D^{\nu(t)} \bar{\Delta}(t),$$

$$Z(t) = [Z_m(t)], \quad Z_m(t) = \begin{cases} 0, & m = 0, 1, \dots, \mathcal{M} - 1, \\ \delta_{\mathcal{M},k}^\lambda \frac{\Gamma(\mathcal{M}+2)}{\Gamma(\mathcal{M}+2-\nu(t))} t^{\mathcal{M}+1-\nu(t)}, & m = \mathcal{M}, \end{cases}$$

and

$$Y(t) = D^{\nu(t)} W(t),$$

$$Y(t) = [Y_m(t)], \quad Y_m(t) = \begin{cases} 0, & m = 0, 1, \dots, \mathcal{M} - 1, \\ \frac{\delta_{\mathcal{M},k}^\lambda}{\mathcal{M}+2} \frac{\Gamma(\mathcal{M}+3)}{\Gamma(\mathcal{M}+3-\nu(t))} t^{\mathcal{M}+2-\nu(t)}, & m = \mathcal{M}. \end{cases}$$

Additionally, we get

$$D^{\gamma(t)} u(t) \simeq A^T \left(\frac{\Gamma(\lambda + \frac{1}{2})}{\Gamma(2\lambda)} t^{1-\gamma(t)} \bar{\mathbf{Q}}^2 \mathbf{D}\Psi(t) + \bar{\mathbf{Q}}\Theta Z(t) + \Theta Y(t) \right) + \frac{a_1}{\Gamma(2-\gamma(t))} t^{1-\gamma(t)}. \tag{5.5}$$

Finally, to evaluate the approximate solution of the equation in Problem 1, we replace the above results in Eq. (1.1) as follows:

$$\mathcal{F} \left[\begin{array}{l} t, A^T (\bar{\mathbf{Q}}^2 \Psi(t) + \bar{\mathbf{Q}}\Theta \bar{\Delta}(t) + \Theta W(t)) + a_1 t + a_0, \\ A^T (\bar{\mathbf{Q}}\Psi(t) + \Theta \bar{\Delta}(t)) + a_1, \\ A^T \left(\frac{\Gamma(\lambda + \frac{1}{2})}{\Gamma(2\lambda)} t^{2-\nu(t)} \bar{\mathbf{Q}}^2 \mathbf{D}\Psi(t) + \bar{\mathbf{Q}}\Theta Z(t) + \Theta Y(t) \right), \\ A^T \left(\frac{\Gamma(\lambda + \frac{1}{2})}{\Gamma(2\lambda)} t^{1-\gamma(t)} \bar{\mathbf{Q}}^2 \mathbf{D}\Psi(t) + \bar{\mathbf{Q}}\Theta Z(t) + \Theta Y(t) \right) + \frac{a_1}{\Gamma(2-\gamma(t))} t^{1-\gamma(t)} \end{array} \right] = f(t). \tag{5.6}$$

At last, by substituting the nodal collocation points [21] in Eq. (5.6), the problem converts to an algebraic system of equations. This procedure provides the approximate solution of the exact solution. The summary of the numerical method is given explicitly by Algorithm 1 below.

Algorithm 1	The numerical method for the MT-VO-fractional differential equations
Input:	Choose the values of \mathcal{M} and \mathcal{K} .
Step 1:	Expand $u''(t)$ by GWFs.
Step 2:	Obtain the transformation matrix Θ .
Step 3:	Compute the modified operational matrix (MOM) of integration $\bar{\mathbf{Q}}$ and vector $\bar{\Delta}(t)$.
Step 4:	Evaluate the MOM of the VO-fractional derivative of orders $\nu(t)$ and $\gamma(t)$.
Step 5:	Assign the vectors $W(t)$, $Z(t)$ and $Y(t)$.
Step 6:	Solve the system of the nonlinear algebraic equations similar to Eq. (23).
Step 7:	Evaluate the unknown vector A .
Output:	Replace the vector obtained in Step 7 in Eq. (5.3) and compute the approximate solution.

5.2. MT-VO-fractional partial differential equations. In this section, the numerical algorithm for solving Problem 2 will be introduced. First, we expand the third partial derivative $\frac{\partial^3 u(x,t)}{\partial x^2 \partial t}$ by GWFs

$$\frac{\partial^3 u(x,t)}{\partial x^2 \partial t} \simeq \Psi^T(x) U \Psi(t). \tag{5.7}$$

Now, by integrating Eq. (5.7) with respect to t , the following relation is generated:

$$\frac{\partial^2 u(x,t)}{\partial x^2} \simeq \Psi^T(x) U (\bar{\mathbf{Q}}\Psi(t) + \Theta \bar{\Delta}(t)) + \varphi''(x) = \mathbf{X}_2(x,t). \tag{5.8}$$

Also, by integrating Eq. (5.8) two times with respect to t , we conclude

$$\frac{\partial u(x,t)}{\partial x} \simeq (\Psi^T(x) \mathbf{Q}^T + \Delta^T(x) \Theta^T) U (\bar{\mathbf{Q}}\Psi(t) + \Theta \bar{\Delta}(t)) + \varphi'(x) - \varphi'(0) + \frac{\partial u(0,t)}{\partial x} = \mathbf{X}_1(x,t), \tag{5.9}$$



so that, by integrating Eq. (5.9) with respect to x from 0 to 1, the unknown function $\frac{\partial u(0,t)}{\partial x}$ is obtained

$$\begin{aligned} \frac{\partial u(0,t)}{\partial x} &= \rho_1(t) - \rho_0(t) - \left(\left[\int_0^1 \Psi^T(x) dx \right] \mathbf{Q}^T + \left[\int_0^1 \Delta^T(x) dx \right] \mathbf{\Theta}^T \right) U (\bar{\mathbf{Q}}\Psi(t) + \mathbf{\Theta}\bar{\Delta}(t)) \\ &\quad - \varphi(1) + \varphi(0) + \varphi'(0). \end{aligned} \tag{5.10}$$

In addition, we deduce

$$\begin{aligned} u(x,t) &\simeq (\Psi^T(x)\mathbf{Q}^{2T} + \Delta^T(x)\mathbf{\Theta}^T\mathbf{Q}^T + \Delta^T(x)\mathbf{\Theta}^T) U (\bar{\mathbf{Q}}\Psi(t) + \mathbf{\Theta}\bar{\Delta}(t)) \\ &\quad + \varphi(x) - \varphi(0) - x\varphi'(0) + x\frac{\partial u(0,t)}{\partial x} + \rho_0(t) \\ &= (\Psi^T(x)\mathbf{Q}^{2T} + \Delta^T(x)\mathbf{\Theta}^T\mathbf{Q}^T + \Delta^T(x)\mathbf{\Theta}^T) U (\bar{\mathbf{Q}}\Psi(t) + \mathbf{\Theta}\bar{\Delta}(t)) \\ &\quad + \varphi(x) - \varphi(0) - x\varphi'(0) + x \left[\rho_1(t) - \rho_0(t) - \left(\left[\int_0^1 \Psi^T(x) dx \right] \mathbf{Q}^T + \left[\int_0^1 \Delta^T(x) dx \right] \mathbf{\Theta}^T \right) \right. \\ &\quad \left. \times U (\bar{\mathbf{Q}}\Psi(t) + \mathbf{\Theta}\bar{\Delta}(t)) - \varphi(1) + \varphi(0) + \varphi'(0) \right] + \rho_0(t) = \mathbf{X}_0(x,t). \end{aligned} \tag{5.11}$$

Then, with the help of the properties of the VO-fractional Caputo derivative operator and Eq. (5.11), we get

$$\begin{aligned} D_t^{\nu(x,t)} u(x,t) &\simeq (\Psi^T(x)\mathbf{Q}^{2T} + \Delta^T(x)\mathbf{\Theta}^T\mathbf{Q}^T + \Delta^T(x)\mathbf{\Theta}^T) U \left(\frac{\Gamma(\lambda + \frac{1}{2})}{\Gamma(2\lambda)} t^{q-\nu(x,t)} \bar{\mathbf{Q}}\mathbf{D}\Psi(t) + \mathbf{\Theta}Z(t) \right) \\ &\quad + x \left[D_t^{\nu(x,t)} \rho_1(t) - D_t^{\nu(x,t)} \rho_0(t) - \left(\left[\int_0^1 \Psi^T(x) dx \right] \mathbf{Q}^T + \left[\int_0^1 \Delta^T(x) dx \right] \mathbf{\Theta}^T \right) \right. \\ &\quad \left. \times U \left(\frac{\Gamma(\lambda + \frac{1}{2})}{\Gamma(2\lambda)} t^{q-\nu(x,t)} \bar{\mathbf{Q}}\mathbf{D}\Psi(t) + \mathbf{\Theta}Z(t) \right) \right] + D_t^{\nu(x,t)} \rho_0(t) = \mathbf{X}_0^\nu(x,t). \end{aligned} \tag{5.12}$$

Furthermore, according to Eq. (5.8), we have

$$D_t^{\vartheta(x,t)} \left(\frac{\partial^2 u(x,t)}{\partial x^2} \right) \simeq \Psi^T(x) U \left(\frac{\Gamma(\lambda + \frac{1}{2})}{\Gamma(2\lambda)} t^{q-\vartheta(x,t)} \bar{\mathbf{Q}}\mathbf{D}\Psi(t) + \mathbf{\Theta}Z(t) \right) = \mathbf{X}_2^\vartheta(x,t).$$

The combination of the above approximate relations and the equation in Problem 2 can be concluded to be

$$\mathcal{H}(x,t, \mathbf{X}_0(x,t), \mathbf{X}_1(x,t), \mathbf{X}_2(x,t), \mathbf{X}_0^\nu(x,t), \mathbf{X}_0^\gamma(x,t), \mathbf{X}_2^\vartheta(x,t)) = h(x,t). \tag{5.13}$$

By placing the nodal points defined in [21] into Eq. (5.13), we get the following system of algebraic equations:

$$\mathcal{H}(x_i, t_j, \mathbf{X}_0(x_i, t_j), \mathbf{X}_1(x_i, t_j), \mathbf{X}_2(x_i, t_j), \mathbf{X}_0^\nu(x_i, t_j), \mathbf{X}_0^\gamma(x_i, t_j), \mathbf{X}_2^\vartheta(x_i, t_j)) = h(x_i, t_j), \tag{5.14}$$

$$i = 1, 2, \dots, 2^{\mathcal{K}-1}(\mathcal{M}_1 + 1) + 1, \quad j = 1, 2, \dots, 2^{\mathcal{K}-1}(\mathcal{M}_2 + 1) + 1.$$

At last, using Newton’s iterative method, we achieve the approximate solution of the equation in Problem 2. The summary of the numerical technique is mentioned explicitly by Algorithm 2 below.

Algorithm 2	The numerical method for the MT-VO-fractional partial differential equations
Input:	Choose the values of \mathcal{M}_1 , \mathcal{M}_2 and \mathcal{K} .
Step 1:	Expand $\frac{\partial^2 u(x,t)}{\partial x^2 \partial t}$ by GWFs.
Step 2:	Obtain the transformation matrix $\mathbf{\Theta}$.
Step 3:	Compute the modified operational matrices of integration \mathbf{Q} , $\bar{\mathbf{Q}}$ and vectors $\Delta(x)$, $\bar{\Delta}(t)$.
Step 4:	Evaluate the MOM of the VO-fractional derivative of orders $\nu(x,t)$, $\gamma(x,t)$ and $\vartheta(x,t)$.
Step 5:	Assign the vector $Z(t)$.
Step 6:	Solve the system of the nonlinear algebraic equations similar to Eq. (31).
Step 7:	Evaluate the unknown matrix U .
Output:	Replace the vector obtained in Step 7 in Eq. (5.11) and compute the approximate solution.



6. ERROR ESTIMATION

The purpose of this section is to introduce the error analysis of the proposed scheme in the Sobolev space. The norm of integer order $\beta \geq 0$ in the Sobolev space $H^\beta(S)$, $S = (a, b)^d$ with $d = 2$, is defined with the following formula [10]:

$$\|u\|_{H^\beta(S)} = \left(\sum_{r=0}^{\beta} \sum_{i=1}^d \|D_i^r u\|_{L^2(S)}^2 \right)^{\frac{1}{2}},$$

where D_i^r is the r -th derivative of u regarding the i -th variable. To simplify the results, it is also useful to introduce the semi-norm as

$$|u|_{H^{\beta;\mathcal{M}}(S)} = \left(\sum_{r=\min(\beta, \mathcal{M}+1)}^{\mu} \sum_{i=1}^d \|D_i^r u\|_{L^2(S)}^2 \right)^{\frac{1}{2}}.$$

Lemma 6.1. *Let $v : I_n\mathcal{K} \rightarrow \mathbb{R}^2$, $I_n\mathcal{K} = [\frac{n-1}{2\mathcal{K}-1}, \frac{n}{2\mathcal{K}-1}] \times [\frac{n-1}{2\mathcal{K}-1}, \frac{n}{2\mathcal{K}-1}]$ is defined in $H^\beta(I_n\mathcal{K})$. If the function $w : \Omega \rightarrow \mathbb{R}^2$, $\Omega = (-1, 1) \times (-1, 1)$ such that $w(x, t) = v(\frac{1}{2\mathcal{K}}x + \frac{2n-1}{2\mathcal{K}}, \frac{1}{2\mathcal{K}}t + \frac{2n-1}{2\mathcal{K}})$. Then, for all $(x, t) \in \Omega$ and $0 \leq r \leq \beta$, we get*

$$\|D_i^r w\|_{L^2(\Omega)} = 2^{\mathcal{K}(1-r)} \|D_i^r u\|_{L^2(I_n\mathcal{K})}, \quad i = 1, 2. \tag{6.1}$$

Proof. We have

$$\begin{aligned} \|D_i^r w\|_{L^2(\Omega)} &= \left(\int_{-1}^1 \int_{-1}^1 |D_i^r w(x, t)|^2 dxdt \right)^{\frac{1}{2}} \\ &= \left(\int_{-1}^1 \int_{-1}^1 \left| D_i^r w\left(\frac{1}{2\mathcal{K}}x + \frac{2n-1}{2\mathcal{K}}, \frac{1}{2\mathcal{K}}t + \frac{2n-1}{2\mathcal{K}}\right) \right|^2 dxdt \right)^{\frac{1}{2}} \\ &= \left(\int_{I_n\mathcal{K}} \int_{I_n\mathcal{K}} 2^{2\mathcal{K}(1-r)} |D_i^r u(y, z)|^2 dydz \right)^{\frac{1}{2}} = 2^{\mathcal{K}(1-r)} \|D_i^r u\|_{L^2(I_n\mathcal{K})}, \end{aligned} \tag{6.2}$$

where the above results are obtained by the following change of variables:

$$y = \frac{1}{2\mathcal{K}}x + \frac{2n-1}{2\mathcal{K}}, \quad z = \frac{1}{2\mathcal{K}}t + \frac{2n-1}{2\mathcal{K}}.$$

□

Theorem 6.2. *Suppose that $u \in H^\beta(\Delta)$, $\Delta = (0, 1) \times (0, 1)$ with $\beta \geq 1$, $\mathcal{M}_1 = \mathcal{M}_2 = \mathcal{M}$, and $n_1 = n_2 = n$. If*

$$u_{\mathcal{M}_1, \mathcal{M}_2}(x, t) = \sum_{n_1=1}^{2^{\mathcal{K}-1}} \sum_{n_2=1}^{2^{\mathcal{K}-1}} \sum_{m_1=0}^{\mathcal{M}} \sum_{m_2=0}^{\mathcal{M}} a_{n_1 n_2 m_1 m_2} \Psi_{n_1 m_1}(x) \Psi_{n_2 m_2}(t),$$

is the best approximation of u , then

$$\|u - u_{\mathcal{M}_1, \mathcal{M}_2}\|_{L^\infty(\Delta)} \leq C \mathcal{M}^{\frac{1}{2}-\mu} \max_{n=1, 2, \dots, 2^{\mathcal{K}-1}} \left(\sum_{r=\min(\beta, \mathcal{M}+1)}^{\mu} \sum_{i=1}^d 2^{2\mathcal{K}(1-r)} \|D_i^r u\|_{L^2(I_n\mathcal{K})}^2 \right)^{\frac{1}{2}}, \tag{6.3}$$

where C is a positive constant independent of \mathcal{M} .

Proof. According to the maximum norm definition, we have

$$\|u - u_{\mathcal{M}_1, \mathcal{M}_2}\|_{L^\infty(\Delta)} = \max_{n=1, 2, \dots, 2^{\mathcal{K}-1}} \|u - u_{\mathcal{M}_1, \mathcal{M}_2}\|_{L^\infty(I_n\mathcal{K})}. \tag{6.4}$$



In addition, by using change variable roles $x = \frac{1}{2\mathcal{K}}\xi + \frac{2n-1}{2\mathcal{K}}$ and $t = \frac{1}{2\mathcal{K}}\eta + \frac{2n-1}{2\mathcal{K}}$, it can be concluded that

$$\begin{aligned} \|u - u_{\mathcal{M}_1, \mathcal{M}_2}\|_{L^\infty(I_{n\mathcal{K}})} &= \sup_{[x,t] \in I_{n\mathcal{K}}} |u(x,t) - u_{\mathcal{M}_1, \mathcal{M}_2}(x,t)| \\ &= \sup_{[\xi, \eta] \in \Omega} \left| u\left(\frac{1}{2\mathcal{K}}\xi + \frac{2n-1}{2\mathcal{K}}, \frac{1}{2\mathcal{K}}\eta + \frac{2n-1}{2\mathcal{K}}\right) \right. \\ &\quad \left. - u_{\mathcal{M}_1, \mathcal{M}_2}\left(\frac{1}{2\mathcal{K}}\xi + \frac{2n-1}{2\mathcal{K}}, \frac{1}{2\mathcal{K}}\eta + \frac{2n-1}{2\mathcal{K}}\right) \right|. \end{aligned} \tag{6.5}$$

By considering

$$u\left(\frac{1}{2\mathcal{K}}\xi + \frac{2n-1}{2\mathcal{K}}, \frac{1}{2\mathcal{K}}\eta + \frac{2n-1}{2\mathcal{K}}\right) = v(\xi, \eta),$$

and

$$u_{\mathcal{M}_1, \mathcal{M}_2}\left(\frac{1}{2\mathcal{K}}\xi + \frac{2n-1}{2\mathcal{K}}, \frac{1}{2\mathcal{K}}\eta + \frac{2n-1}{2\mathcal{K}}\right) = v_{\mathcal{M}_1, \mathcal{M}_2}(\xi, \eta),$$

on the interval Ω , we deduce

$$\begin{aligned} \|u - u_{\mathcal{M}_1, \mathcal{M}_2}\|_{L^\infty(I_{n\mathcal{K}})} &= \sup_{[\xi, \eta] \in \Omega} |v(\xi, \eta) - v_{\mathcal{M}_1, \mathcal{M}_2}(\xi, \eta)| \\ &= \|v - v_{\mathcal{M}_1, \mathcal{M}_2}\|_{L^\infty(\Omega)}. \end{aligned} \tag{6.6}$$

On the other hand, from [10], we have

$$\|v - v_{\mathcal{M}_1, \mathcal{M}_2}\|_{L^\infty(\Omega)} \leq C\mathcal{M}^{\frac{1}{2}-\beta} |v|_{H^{\beta; \mathcal{M}}(\Omega)}. \tag{6.7}$$

Also, from Lemma 1, we obtain

$$\begin{aligned} |v|_{H^{\beta; \mathcal{M}}(\Omega)} &= \left(\sum_{r=\min(\beta, \mathcal{M}+1)}^{\beta} \sum_{i=1}^d \|D_i^r v\|_{L^2(\Omega)}^2 \right)^{\frac{1}{2}} \\ &= \left(\sum_{r=\min(\beta, \mathcal{M}+1)}^{\beta} \sum_{i=1}^d 2^{2\mathcal{K}(1-r)} \|D_i^r u\|_{L^2(I_{n\mathcal{K}})}^2 \right)^{\frac{1}{2}}. \end{aligned} \tag{6.8}$$

Therefore, we conclude

$$\|u - u_{\mathcal{M}_1, \mathcal{M}_2}\|_{L^\infty(I_{n\mathcal{K}})} \leq C\mathcal{M}^{\frac{1}{2}-\beta} \left(\sum_{r=\min(\beta, \mathcal{M}+1)}^{\beta} \sum_{i=1}^d 2^{2\mathcal{K}(1-r)} \|D_i^r u\|_{L^2(I_{n\mathcal{K}})}^2 \right)^{\frac{1}{2}}. \tag{6.9}$$

Finally, by combining Eqs. (6.4) and (6.9), the desired result is achieved. □

Corollary 6.3. *Regarding the assumptions of the previous theorem and by considering $\beta \geq 1, d = 2$, and $\mathcal{M} \geq \beta - 1$, we infer*

$$\|u - u_{\mathcal{M}_1, \mathcal{M}_2}\|_{L^\infty(\Delta)} \leq C\mathcal{M}^{\frac{1}{2}-\beta} 2^{2\mathcal{K}(1-\beta)} \max_{n=1,2,\dots,2\mathcal{K}-1} \left(\sum_{i=1}^d \|D_i^\mu u\|_{L^2(I_{n\mathcal{K}})}^2 \right)^{\frac{1}{2}}. \tag{6.10}$$

From this result, it can be seen that by increasing the values of \mathcal{M} and \mathcal{K} , the error tends to zero.



TABLE 1. The absolute errors for diverse values of \mathcal{K} , $\nu(t)$, and $\gamma(t)$ with $\mathcal{M} = 5$ of Example 7.1.

t	$\nu(t) = 2 - \sin^2(t), \gamma(t) = 1 - 0.5 \exp(-t)$		$\nu(t) = \frac{15 - \sin^5(t)}{10}, \gamma(t) = \frac{3(\sin(t) + \cos(t))}{5}$	
	$\mathcal{K} = 1$	$\mathcal{K} = 2$	$\mathcal{K} = 1$	$\mathcal{K} = 2$
0.1	1.6710×10^{-13}	5.2043×10^{-18}	8.7196×10^{-13}	6.6296×10^{-18}
0.2	1.0545×10^{-13}	4.7129×10^{-17}	1.2609×10^{-12}	8.1438×10^{-18}
0.3	4.3564×10^{-14}	1.7330×10^{-16}	1.6094×10^{-12}	6.2401×10^{-17}
0.4	1.7005×10^{-14}	4.1160×10^{-16}	1.9153×10^{-12}	5.9443×10^{-16}
0.5	7.4424×10^{-14}	7.4106×10^{-16}	2.1793×10^{-12}	2.6322×10^{-15}
0.6	1.2681×10^{-13}	3.0957×10^{-14}	2.4046×10^{-12}	4.6165×10^{-15}
0.7	1.7258×10^{-13}	1.3039×10^{-13}	2.5962×10^{-12}	3.9902×10^{-15}
0.8	2.1080×10^{-13}	3.0741×10^{-13}	2.7603×10^{-12}	8.7256×10^{-16}
0.9	2.4177×10^{-13}	5.4943×10^{-13}	2.9036×10^{-12}	4.3534×10^{-15}
0.9	2.6768×10^{-13}	7.9712×10^{-13}	3.0318×10^{-12}	9.7541×10^{-15}

7. NUMERICAL EXAMPLES

In this section, we implement the numerical approach in several numerical tests in order to demonstrate the efficiency and applicability of the scheme.

Example 7.1. Consider the following multi-term variable-order fractional differential equation [27]:

$$D_t^{\nu(t)} u(t) + \sin(t) D_t^{\gamma(t)} u(t) + \cos(t) u(t) = \frac{6t^{3-\nu(t)}}{\Gamma(4-\nu(t))} + \frac{6 \sin(t) t^{3-\gamma(t)}}{\Gamma(4-\gamma(t))} + t^3 \cos(t), \quad 1 < \nu(t) \leq 2, \quad 0 < \gamma(t) \leq 1,$$

with conditions $u(0) = u'(0) = 0$. The exact solution to this problem is $u(t) = t^3$. Regarding the proposed method explained in the previous section, we listed the absolute error for diverse values of \mathcal{K} , $\nu(t)$, and $\gamma(t)$ in Table 1. This table demonstrates that by increasing the number of divisions of the interval $[0, 1]$, the approximate solution becomes more accurate.

Example 7.2. Consider the following nonlinear multi-term variable-order fractional differential equation [12]:

$$D_t^{\gamma(t)} u(t) - 6D_t^{\nu(t)} u(t)u(t) - 7u'(t) + 5u(t) = f(t), \quad 1 < \nu(t) \leq 2, \quad 0 < \gamma(t) \leq 1,$$

where

$$f(t) = -150 \left(\frac{2}{\Gamma(3-\nu(t))} t^{2-\nu(t)} \right) (3t + t^2) + \frac{15}{\Gamma(2-\gamma(t))} t^{1-\gamma(t)} + \frac{10}{\Gamma(3-\gamma(t))} t^{2-\gamma(t)} - 7(15 + 10t) + 25(3t + t^2).$$

with conditions $u(0) = 0$ and $u'(0) = 15$. The exact solution to this problem is $u(t) = 5(3t + t^2)$. In view of the proposed scheme and taking $\mathcal{M} = \mathcal{K} = 2$ and $\gamma(t) = \frac{3(\sin(t) + \cos(t))}{5}$, we get

$$u(t) = \begin{cases} -1.8717912557 \times 10^{-14} t^4 + 6.0026619918 \times 10^{-15} t^3 + 5t^2 + 15t, & 0 \leq t < \frac{1}{2}, \\ 9.17181561835 \times 10^{-15} t^4 - 2.0485000330 \times 10^{-14} t^3 + 5t^2 \\ + 15.0000000000000059t - 1.39259154772 \times 10^{-15}, & \frac{1}{2} \leq t < 1. \end{cases}$$

In addition, the absolute errors for diverse values of $\nu(t)$ with $\mathcal{M} = \mathcal{K} = 2$ and $\gamma(t) = \frac{3(\sin(t) + \cos(t))}{5}$ are presented in Table 2. This table illustrates that the performance of our method is far better compared with the Legendre wavelet method [12].

Example 7.3. Consider the following multi-term variable-order fractional differential equation [23]:

$$pD_t^{\nu(t)} u(t) + qD_t^{\gamma(t)} u(t) + ru(t) = f(t), \quad 1 < \nu(t) \leq 2, \quad 0 < \gamma(t) \leq 1,$$



TABLE 2. The absolute errors for diverse values of $\nu(t)$ with $\mathcal{M} = \mathcal{K} = 2$ and $\gamma(t) = \frac{3(\sin(t)+\cos(t))}{5}$ of Example 7.2.

t	Present method		Legendre wavelet method [12]
	$\nu(t) = 2$	$\nu(t) = 2 - \cos^2(t)$	$\nu(t) = 2$
0.2	1.3497×10^{-16}	1.7147×10^{-17}	1.199041×10^{-14}
0.4	6.4057×10^{-16}	3.3255×10^{-14}	1.421085×10^{-14}
0.6	4.4567×10^{-16}	5.5473×10^{-16}	2.842171×10^{-14}
0.8	3.2767×10^{-15}	1.3024×10^{-15}	1.669775×10^{-13}
1	1.1534×10^{-14}	2.1454×10^{-15}	2.273737×10^{-13}

TABLE 3. Comparison of the absolute error obtained by the presented method, the Legendre wavelet method [12], and the collocation spectral method [23] with different values of \mathcal{K} of Case 1 for Example 7.3.

t	Present method		Legendre wavelet method [12]	Collocation spectral method [23]
	$\mathcal{M} = 2, \mathcal{K} = 1$	$\mathcal{M} = 2, \mathcal{K} = 2$	$M = 4, k = 2$	$n = 2$
0.2	4.4145×10^{-17}	5.9798×10^{-17}	8.091305×10^{-12}	2.425319×10^{-12}
0.4	3.0204×10^{-16}	1.0580×10^{-16}	2.024535×10^{-9}	2.425319×10^{-12}
0.6	8.4687×10^{-16}	6.0328×10^{-16}	9.564669×10^{-10}	2.425319×10^{-12}
0.8	1.5984×10^{-15}	1.0345×10^{-14}	1.696030×10^{-10}	2.425319×10^{-12}
1	2.3232×10^{-15}	3.2685×10^{-14}	1.734222×10^{-10}	2.425319×10^{-12}

with conditions $u(0) = u_0, u'(0) = u_1$.

Case 1: Let

$$p = 1, \quad q = -10, \quad r = 1, \quad u_0 = 5, \quad u_1 = 10, \quad \nu(t) = \frac{t + 2 \exp(t)}{7}, \quad \gamma(t) = 1,$$

and

$$f(t) = 10 \left(\frac{t^{2-\nu(t)}}{\Gamma(3-\nu(t))} + \frac{t^{1-\nu(t)}}{\Gamma(2-\nu(t))} \right) + 5t^2 - 90t - 95.$$

The exact solution to this problem is $u(t) = 5(1+t)^2$. By considering the technique described in Section 5 and the parameters mentioned in Case 1, the absolute errors for different values of \mathcal{K} are shown in Table 3. Also, from Table 3, it can be seen that our scheme, in comparison to the Legendre wavelet method [12] and the collocation spectral method [23], is more accurate.

Case 2: By considering [40]

$$p = 1, \quad q = 2, \quad r = 4, \quad u_0 = u_1 = 0, \quad \nu(t) = 2, \quad \gamma(t) = 1,$$

and

$$f(t) = 2 + 4t + 4t^2,$$

the damped mechanical oscillator equation is obtained. The exact solution to this problem is $u(t) = t^2$. The components of this equation are defined in Table 4. For $\mathcal{M} = 2$ and $\mathcal{K} = 1$, we get

$$A = [2, 0, 0].$$

Then, the approximate solution based on the proposed method is as follows:

$$u(t) = t^2,$$

which is the exact solution of the problems.



TABLE 4. The components of the damped mechanical oscillator equation.

t	Time
r	Spring stiffness
$f(t)$	External force
p	Mass of the particle attached to the spring
q	Measure of the strength of the damper
$u(t)$	Displacement of the mass from its rest position

TABLE 5. Comparison of the maximum absolute error obtained by the presented method and the methods in [1, 43] with $\nu(x, t) = 1$ and $\gamma(x, t) = 0.8 + 0.005 \sin(x) \cos(xt)$ of Example 7.4.

	Present method ($\mathcal{M}_1 = \mathcal{M}_2 = 1$)	
	$\mathcal{K} = 1$	$\mathcal{K} = 2$
L_∞ -error	1.8423×10^{-16}	1.0173×10^{-15}
CPU	3.8059×10^{-1}	2.1266
Method in [1]		
$N = M$	$\theta_1 = \vartheta_1 = \frac{1}{2}, \theta_2 = \vartheta_2 = 0$	$\theta_1 = \vartheta_1 = \frac{1}{2}, \theta_2 = \vartheta_2 = \frac{1}{2}$
6	1.249×10^{-16}	2.9143×10^{-16}
10	9.5314×10^{-17}	1.4898×10^{-16}
Method in [43]		
$h = \tau$	$\frac{1}{200}$	$\frac{1}{400}$
L_∞ -error	2.5613×10^{-3}	1.2781×10^{-3}

Example 7.4. Consider the VO-fractional mobile-immobile advection-dispersion equation in the following form [1, 43]:

$$D_t^{\nu(x,t)}u(x, t) + D_t^{\gamma(x,t)}u(x, t) = \frac{\partial^2 u(x, t)}{\partial x^2} - \frac{\partial u(x, t)}{\partial x} - 5(x - 1)x \frac{t^{1-\gamma(x,t)}}{\Gamma(2 - \gamma(x, t))} - 5(2xt - 3t + x^2 + x - 3), \quad 0 < \nu(x, t), \gamma(x, t) \leq 1,$$

subject to the initial and boundary conditions

$$u(x, 0) = 5x - 5x^2, \quad u(0, t) = u(1, t) = 0, \quad x \in [0, 1], \quad t \in [0, 1].$$

The exact solution to this problem in the case when $\nu(x, t) = 1$ is $u(x, t) = 5(t + 1)x(1 - x)$. By applying the proposed approach with $\mathcal{M}_1 = \mathcal{M}_2 = \mathcal{K} = 1$ and $\nu(x, t) = \gamma(x, t) = 1$, we have

$$u_{11} = -10, \quad u_{12} = -4.948402911835508 \times 10^{-16},$$

$$u_{21} = -1.7460985751571553 \times 10^{-15}, \quad u_{22} = -1.1708093942297388 \times 10^{-15}.$$

Then, the approximate solution is obtained as follows:

$$u(x, t) = 5x - 5tx^2 + 8.1349455915 \times 10^{-17}tx^3 + 5xt + 6.63834914181 \times 10^{-17}x^2t^2 - 2.92702348 \times 10^{-16}t^2x^3 - 3.71132565 \times 10^{-16}t^2x - 5x^2.$$

Also, in Table 5, we compare the outcomes of the present method to the methods in [1, 43]. As can be seen in Table 5, the current method with a few terms of basis functions provides good results. Moreover, Figure 2 shows that when the function of $\nu(x, t)$ approaches 1, the approximate solution is close to the analytical solution.



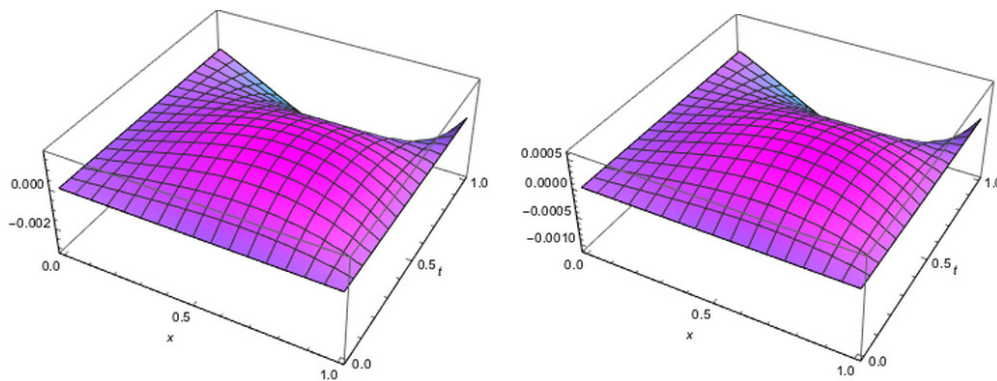


FIGURE 2. The absolute error for $\nu(x, t) = 1 - 0.06 \sin(\pi xt)$ (left) and $\nu(x, t) = 1 - 0.02 \sin(\pi xt)$ (right) with $\mathcal{M}_1 = \mathcal{M}_2 = \mathcal{K} = 1$ and $\gamma(x, t) = 0.8 + 0.005 \sin(x) \cos(xt)$ of Example 7.4.

TABLE 6. Errors and CPU time for different values of $\vartheta(x, t)$ and $\gamma(x, t)$ with $\mathcal{M}_2 = 2$ and $\mathcal{K} = 1$ for Example 7.5.

	$\vartheta(x, t) = \frac{9-x^2+t^3}{120}, \gamma(x, t) = \frac{15+\sin^2(xt)}{16}$		
	$\mathcal{M}_1 = 3$	$\mathcal{M}_1 = 5$	$\mathcal{M}_1 = 8$
L_2 -error	1.1883×10^{-3}	1.2796×10^{-5}	3.0154×10^{-10}
L_∞ -error	8.2396×10^{-4}	1.1395×10^{-5}	2.4487×10^{-10}
CPU	4.4182×10^{-1}	7.2397×10^{-1}	9.5284×10^{-1}
	$\vartheta(x, t) = \gamma(x, t) = \frac{9-\sin(xt)}{10}$		
	$\mathcal{M}_1 = 3$	$\mathcal{M}_1 = 5$	$\mathcal{M}_1 = 8$
L_2 -error	1.0622×10^{-3}	1.2226×10^{-5}	2.9046×10^{-10}
L_∞ -error	7.6064×10^{-4}	1.0594×10^{-5}	2.4480×10^{-10}
CPU	4.0886×10^{-1}	5.0404×10^{-1}	6.3835×10^{-1}

Example 7.5. Consider the multi-term VO-fractional cable equation in the following form:

$$\frac{\partial u(x, t)}{\partial t} = D_t^{1-\vartheta(x, t)} \left(\frac{\partial^2 u(x, t)}{\partial x^2} \right) - D_t^{1-\gamma(x, t)} u(x, t) + 2 \left(t + \frac{\pi^2 t^{\vartheta(x, t)+1}}{\Gamma(2 + \vartheta(x, t))} + \frac{t^{\gamma(x, t)+1}}{\Gamma(2 + \gamma(x, t))} \right) \sin(\pi x), \quad 0 < \vartheta(x, t), \gamma(x, t) \leq 1,$$

subject to the initial and boundary conditions

$$u(x, 0) = u(0, t) = u(1, t) = 0, \quad x \in [0, 1], \quad t \in [0, 1].$$

The exact solution to this problem is $u(x, t) = t^2 \sin(\pi x)$. The results of this problem are presented in Table 6 and Figure 3. Regarding the method, the L_2 -error and L_∞ -error for different values of $\vartheta(x, t)$ and $\gamma(x, t)$ with $\mathcal{M}_2 = 2$ and $\mathcal{K} = 1$ are displayed in Table 6. From Table 6, it is clear that the approximate solutions converge to the exact solution when the number of basis functions \mathcal{M}_1 is increased. Also, the absolute error and contour plot with $\mathcal{M}_1 = 5, \mathcal{M}_2 = 2, \mathcal{K} = 1$, and $\vartheta(x, t) = \gamma(x, t) = 0.5$ are demonstrated in Figure 3.



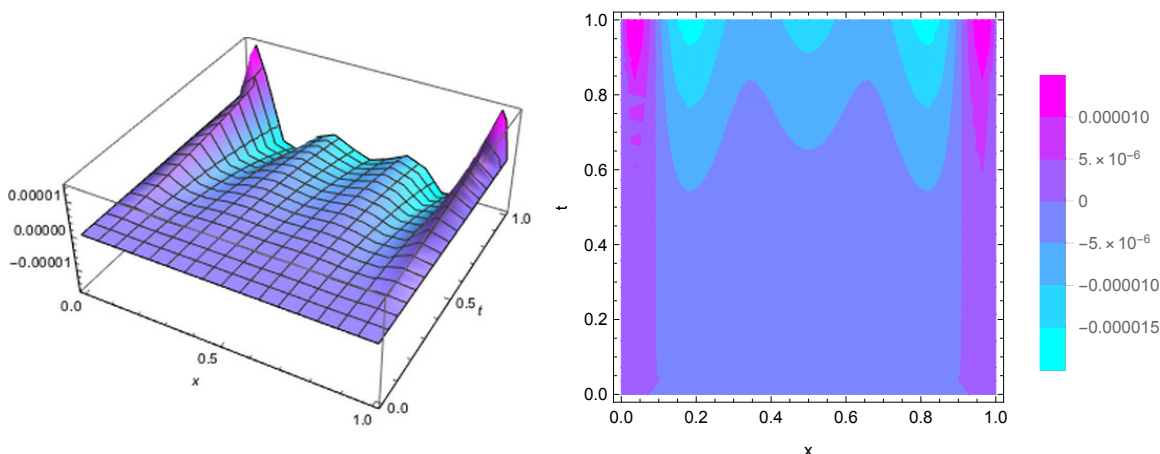


FIGURE 3. The absolute error (left) and the contour plot (right) with $\mathcal{M}_1 = 5$, $\mathcal{M}_2 = 2$, $\mathcal{K} = 1$, and $\vartheta(x, t) = \gamma(x, t) = 0.5$ of Example 7.5.

Example 7.6. Consider the VO-fractional nonlinear Galilei invariant advection-diffusion equation in the following form [2, 14]:

$$D_t^{\nu(x,t)}u(x, t) + \frac{\partial u(x, t)}{\partial x} = D_t^{1-\vartheta(x,t)} \left(\frac{\partial^2 u(x, t)}{\partial x^2} \right) + u(x, t) - (u(x, t))^2 + t \exp(t) \left(2 + t^3 \exp(t) - \frac{2t^{1+\vartheta(x,t)}}{\Gamma(2 + \vartheta(x, t))} \right),$$

$$0 < \nu(x, t), \vartheta(x, t) \leq 1,$$

subject to the initial and boundary conditions

$$u(x, 0) = 0, \quad u(0, t) = t^2, \quad u(1, t) = t^2 \exp(x), \quad x \in [0, 1], \quad t \in [0, 1].$$

The exact solution to this problem in the case when $\nu(x, t) = 1$ is $u(x, t) = t^2 \exp(x)$.

Case 1: Assume that the VO-fractional derivatives in this example are

$$\nu(x, t) = 1, \quad \vartheta(x, t) = \frac{1}{300}(10 - tx).$$

According to the parameters defined in this part, we provide the maximum absolute error for diverse values of \mathcal{M}_1 in Table 7. According to the obtained results in this table, it can be understood that the proposed method with a few terms of basis functions has high accuracy in comparison to methods in [2, 14].

Case 2: Let

$$\nu(x, t) = \nu, \quad \vartheta(x, t) = \frac{1}{100}(\exp(-xt)).$$

In this part, the approximate solution for different values of ν with $\mathcal{M}_1 = 5$, $\mathcal{M}_2 = 2$, and $\mathcal{K} = 1$ is illustrated in Table 8. Also, Table 8 indicates that when the values of ν approach 1 the approximate solution are close to the analytical solution. Moreover, the absolute error and the contour plot for $\mathcal{M}_1 = 5$, $\mathcal{M}_2 = 2$, and $\mathcal{K} = 1$ with $\nu = 1$ are shown in Figure 4.

Case 3: Suppose that

$$\nu(x, t) = 1, \quad \vartheta(x, t) = \frac{1}{500}((tx)^2 - (\sin(tx))^3 + (\cos(tx))^4 + 16).$$

The absolute error for $\mathcal{M}_1 = \mathcal{M}_2 = 2$ and $\mathcal{K} = 2$ is plotted in Figure 5.



TABLE 7. Comparison of the maximum absolute error obtained by the presented method and the methods in [2, 14] with $\mathcal{M}_2 = 2$ and $\mathcal{K} = 1$ of Case 1 for Example 7.6.

$\mathcal{M}_2 = 2, \mathcal{K} = 1$	Present method		
	$\mathcal{M}_1 = 2$	$\mathcal{M}_1 = 5$	$\mathcal{M}_1 = 8$
	2.3739×10^{-5}	2.1772×10^{-9}	3.6008×10^{-14}
$(\alpha_1, \beta_1, \alpha_2, \beta_2)$	Method in [2]		
	$M = N = 2$	$M = N = 5$	$M = N = 10$
(0, 0, 0, 0)	1.36248×10^{-3}	5.42912×10^{-8}	2.66454×10^{-14}
(0.5, 0.5, 0, 0)	1.36248×10^{-3}	4.08291×10^{-8}	2.62013×10^{-14}
(-0.5, 0, 0.5, 0.5)	1.26147×10^{-2}	7.07546×10^{-8}	3.57712×10^{-14}
	Method in [14]		
	$h_t = h_x^2 = \frac{1}{16}$	$h_t = h_x^2 = \frac{1}{64}$	$h_t = h_x^2 = \frac{1}{256}$
—	5.5308×10^{-4}	1.4567×10^{-4}	6.1896×10^{-5}

TABLE 8. The approximate solution for different values of ν with $\mathcal{M}_1 = 5$, $\mathcal{M}_2 = 2$, and $\mathcal{K} = 1$ of Case 2 for Example 7.6.

$x = t$	0.8	0.85	0.9	0.95	1
0.1	1.14931×10^{-2}	1.14089×10^{-2}	1.13083×10^{-2}	1.11898×10^{-2}	1.10517×10^{-2}
0.3	1.26739×10^{-1}	1.25603×10^{-1}	1.24353×10^{-1}	1.22984×10^{-1}	1.21487×10^{-1}
0.5	4.26435×10^{-1}	4.23202×10^{-1}	4.19755×10^{-1}	4.16084×10^{-1}	4.12180×10^{-1}
0.7	1.00735	1.00255	9.97526×10^{-1}	9.92255×10^{-3}	9.86738×10^{-1}
0.9	0.00538	2.00227	1.99905	1.99576	1.99227

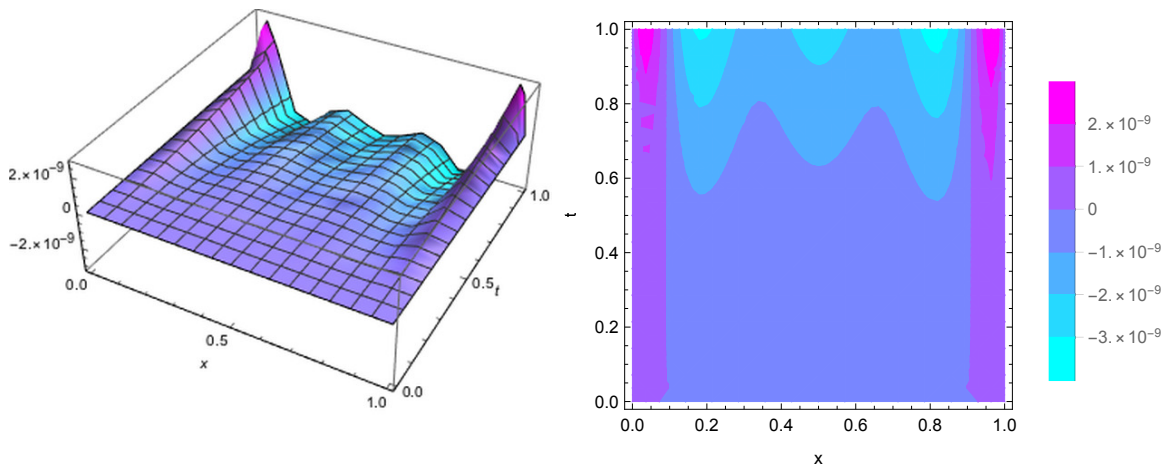


FIGURE 4. The absolute error (left) and the contour plot (right) for Case 2 with $\mathcal{M}_1 = 5$, $\mathcal{M}_2 = 2$, and $\mathcal{K} = 1$ of Example 7.6.

8. CONCLUSION

In this work, we have provided the discretization method by means of the Gegenbauer wavelet functions for the multi-term variable-order fractional partial differential equations. We also introduce an efficient method for calculating



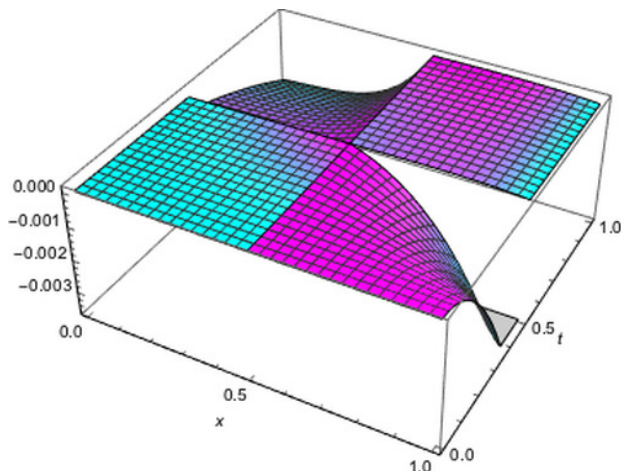


FIGURE 5. The absolute error for Case 3 with $\mathcal{M}_1 = \mathcal{M}_2 = 2$ and $\mathcal{K} = 2$ of Example 7.6.

operational matrix that play a major role in the numerical method. Besides, the modified operational matrices elements are provided explicitly, and this in turn greatly simplifies the process of obtaining approximate solutions. Also, we have discussed and analyzed the error of the approximate function in Sobolev space. Finally, we have applied the theory of numerical technique to several examples to affirm the validity of our claim. It is worth mentioning here that the proposed approach is a powerful tool to produce a reliable approximate solution for the problems with a few terms of GWFs.

ACKNOWLEDGMENT

We express our sincere thanks to the anonymous referees for their valuable suggestions that improved the final manuscript.

REFERENCES

- [1] M. A. Abdelkawy, M. A. Zaky, A. H. Bhrawy, and D. Baleanu, *Numerical simulation of time variable fractional order mobile-immobile advection-dispersion model*, Rom. Rep. Phys., *67*(3) (2015), 773–791.
- [2] M. A. Abd-Elkawy and R. T. Alqahtani, *Space-time spectral collocation algorithm for the variable-order Galilei invariant advection diffusion equations with a nonlinear source term*, Math. Model. Anal., *22*(1) (2017), 1–20.
- [3] O. A. Arqub and B. Maayah, *Adaptive the Dirichlet model of mobile/immobile advection/dispersion in a time-fractional sense with the reproducing kernel computational approach: Formulations and approximations*, Int. J. Mod. Phys. B., *37*(18) (2023), 2350179.
- [4] O. A. Arqub, *Computational algorithm for solving singular Fredholm time-fractional partial integrodifferential equations with error estimates*, J. Appl. Math. Comput., *59*(1) (2019), 227–243.
- [5] O. A. Arqub and N. Shawagfeh, *Application of reproducing kernel algorithm for solving Dirichlet time-fractional diffusion-Gordon types equations in porous media*, J. Porous. Media., *22*(4) (2019), 411–434.
- [6] A. Babaaghaie and K. Maleknejad, *Numerical solutions of nonlinear two-dimensional partial Volterra integro-differential equations by Haar wavelet*, J. Comput. Appl. Math., *317* (2017), 643–651.
- [7] R. Bagley and P. Torvik, *A theoretical basis for the application of fractional calculus to viscoelasticity*, J. Rheol., *27* (1983), 201–210.
- [8] R. L. Bagley and P. J. Torvik, *Fractional calculus in the transient analysis of viscoelastically damped structures*, AIAA J., *23* (1985), 918–925.
- [9] R. T. Baillie, *Long memory processes and fractional integration in econometrics*, J. Econometrics., *73* (1996), 5–59.



- [10] C. Canuto, M. Y. Hussaini, A. Quarteroni, and T. A. Zang, *Spectral methods*, New York, NY: Springer, 2006.
- [11] W. Chen, J. Zhang, and J. Zhang, *A variable-order time fractional derivative model for chloride ions sub-diffusion in concrete structures*, *Fract. Calc. Appl. Anal.*, *16*(1) (2013), 76–92.
- [12] Y. M. Chen, Y. Q. Wei, D. Y. Liu, and H. Yu, *Numerical solution for a class of nonlinear variable-order fractional differential equations with Legendre wavelets*, *Appl. Math. Lett.*, *46* (2015), 83–88.
- [13] M. Q. Chen, C. Hwang, and Y. P. Shih, *The computation of wavelet-Galerkin approximation on a bounded interval*, *Int. J. Numer. Methods Eng.*, *39* (1996), 2921–2944.
- [14] C. M. Chen, F. Liu, V. Anh, and I. Turner, *Numerical simulation for the variable-order Galilei invariant advection diffusion equation with a nonlinear source term*, *Appl. Math. Comput.*, *217*(12) (2011), 5729–5742.
- [15] C. F. M. Coimbra, *Mechanics with variable-order differential operators*, *Ann. Phys.*, *12*(11–12) (2003), 692–703.
- [16] G. R. J. Cooper and D.R. Cowan, *Filtering using variable-order vertical derivatives*, *Comput. Geosci.*, *30*(5) (2004), 455–459.
- [17] C. Chui, *Wavelets: a mathematical tool for signal analysis*, SIAM, 1997.
- [18] H. Dehestani, Y. Ordokhani, and M. Razzaghi, *Fractional-order Bessel wavelet functions for solving variable-order fractional optimal control problems with estimation error*, *Int. J. Syst. Sci.*, *51*(6) (2020), 1032–1052.
- [19] H. Dehestani and Y. Ordokhani, *Designing an efficient algorithm for fractional partial integro-differential viscoelastic equations with weakly singular kernel*, *CMDE*, *13*(1) (2025), 214–232.
- [20] H. Dehestani, Y. Ordokhani, and M. Razzaghi, *Application of the modified operational matrices in multiterm variable-order time-fractional partial differential equations*, *Math. Meth. Appl. Sci.*, *42* (2019), 7296–7313.
- [21] H. Dehestani, Y. Ordokhani, and M. Razzaghi, *Application of fractional Gegenbauer functions in variable-order fractional delay-type equations with non-singular kernel derivatives*, *Chaos Solitons Fractals.*, *140* (2020), 110111.
- [22] K. Diethelm and A. D. Freed, *On the solution of nonlinear fractional-order differential equations used in the modeling of viscoplasticity*, in: *Scientific Computing in Chemical Engineering II*, Springer, (1999), 217–224.
- [23] A. A. El-Sayed and P. Agarwal, *Numerical solution of multiterm variable-order fractional differential equations via shifted Legendre polynomials*, *Math. Meth. Appl. Sci.*, *42*(11) (2019), 3978–3991.
- [24] M. S. Hashemi, E. Ashpazzadeh, M. Moharrami, and M. Lakestani, *Fractional order Alpert multiwavelets for discretizing delay fractional differential equation of pantograph type*, *Appl. Numer. Math.*, *170* (2021), 1–13.
- [25] B. Hussain, A. Afroz, and A. Abdullah, *Haar wavelet based numerical method for solving proportional delay variant of Dirichlet boundary value problems*, *IJNAA.*, *14*(1) (2023), 287–298.
- [26] M. H. Heydari, A. Atangana, Z. Avazzadeh, and M.R. Mahmoudi, *An operational matrix method for nonlinear variable-order time fractional reaction–diffusion equation involving Mittag-Leffler kernel*, *Eur. Phys. J. Plus.*, *135*(2) (2020), 1–19.
- [27] M. H. Heydari, M. R. Hooshmandasl, C. Cattani, and G. Hariharan, *An optimization wavelet method for multi variable-order fractional differential equations*, *Fundam. Inform.*, *151*(1–4) (2017), 255–273.
- [28] J. Jia, X. Zheng, H. Fu, P. Dai, and H. Wang, *A fast method for variable-order space-fractional diffusion equations*, *Numer. Algor.*, *85*(4D) (2020), 1519–1540.
- [29] X. Li and B. Wu, *A new reproducing kernel method for variable-order fractional boundary value problems for functional differential equations*, *J. Comput. Appl. Math.*, *311* (2017), 387–393.
- [30] F. Mainardi, *Fractional calculus: some basic problems in continuum and statistical mechanics*, in: *Fractals and Fractional Calculus in Continuum Mechanics* (Udine, 1996), in: *CISM Courses and Lect.*, Springer, Vienna, *378* (1997), 291–348.
- [31] H. T. C. Pedro, M. H. Kobayashi, J. M. C. Pereira, and C. F. M. Coimbra, *Variable-order modeling of diffusive-convective effects on the oscillatory flow past a sphere*, *J. Vib. Control.*, *14*(9–10) (2008), 1659–1672.
- [32] L. E. S. Ramirez and C. F. M. Coimbra, *A variable-order constitutive relation for viscoelasticity*, *Ann. Phys.*, *16*(7–8) (2007), 543–552.
- [33] Y. A. Rossikhin and M. V. Shitikova, *Applications of fractional calculus to dynamic problems of linear and nonlinear hereditary mechanics of solids*, *Appl. Mech. Rev.*, *50* (1997), 15–67.
- [34] S. G. Samko and B. Ross, *Integration and differentiation to a variable fractional order*, *Integral Transforms Spec. Funct.*, *1*(4) (1993), 277–300.



- [35] H. G. Sun, W. Chen, H. Sheng, and Y. Q. Chen, *Onmean square displacement behaviors of anomalous diffusions with variable and random orders*, Phys. Lett. A., *374* (2010), 906–910.
- [36] M. Tavassoli Kajania, M. Ghasemi, and E. Babolian, *Comparison between the homotopy perturbation method and the sine-cosine wavelet method for solving linear integro-differential equations*, Comput. Math. Appl., *54* (2007), 1162–1168.
- [37] C. Tseng, *Design of variable and adaptive fractional order FIR differentiators*, Signal Process., *86*(10) (2006), 2554–2566.
- [38] M. Usman, M. Hamid, R. U. Haq, and W. Wang, *An efficient algorithm based on Gegenbauer wavelets for the solutions of variable-order fractional differential equations*, Eur. Phys. J. Plus., *133* (2018), 327.
- [39] M. Usman, M. Hamid, T. Zubair, R. U. Haq, W. Wang, and M. B. Liu, *Novel operational matrices-based method for solving fractional-order delay differential equations via shifted Gegenbauer polynomials*, Appl. Math. Comput., *372* (2020), 124985.
- [40] K. Veselic, *Damped oscillations of linear systems-A mathematical introduction*, Springer, 2011.
- [41] S. Yaghoobi, B. Parsa Moghaddam, and K. Ivaz, *An efficient cubic spline approximation for variable-order fractional differential equations with time delay*, Nonlinear. Dyn., *87*(2) (2017), 815–826.
- [42] H. Zhang, F. Liu, P. Zhuang, I. Turner, and V. Anh, *Numerical analysis of a new space-time variable fractional order advection dispersion equation*, Appl. Math. Comput., *242* (2014), 541–550.
- [43] H. Zhang, F. Liu, M. S. Phanikumar, and M. M. Meerschaert, *A novel numerical method for the time variable fractional order mobile-immobile advection-dispersion model*, Comput. Math. Appl., *66*(5) (2013), 693–701.

